



PCCP

Relationship Between Asymmetric Magnetoresistive Effect and Magnetocaloric Effect in Ni₄₃Co₇Mn_{39-x}Cr_xSn₁₁ Heusler Alloys

Journal:	<i>Physical Chemistry Chemical Physics</i>
Manuscript ID	CP-ART-01-2019-000145.R1
Article Type:	Paper
Date Submitted by the Author:	06-Mar-2019
Complete List of Authors:	<p>Xu, Yunli; China Three Gorges University, College of Science Yang, Dongchao; China Three Gorges University, Research Institute for Magnetolectronics & Weak Magnetic-field Detection, College of Science Ding, Linjie; China Three Gorges University, Research Institute for Magnetolectronics & Weak Magnetic-field Detection, College of Science Yi, Lizhi; China Three Gorges University, Research Institute for Magnetolectronics & Weak Magnetic-field Detection, College of Science Fan, S. W.; China Three Gorges University, Physics Pan, Liqing; China Three Gorges University, , College of Science and Research Institute for New Energy Li, Jia; Institute of Physics,CAS, China, State key Lab for magnetism Hu, Fengxia; Institute of Physics,CAS, China, State key Lab for magnetism Yu, Guanghua; University of Science and Technology Beijing, Department of Material Physics and Chemistry Xiao, John Q; University of Delaware, Department of Physics and Astronomy</p>

SCHOLARONE™
Manuscripts

Relationship Between Asymmetric Magnetoresistive Effect and Magnetocaloric Effect in $\text{Ni}_{43}\text{Co}_7\text{Mn}_{39-x}\text{Cr}_x\text{Sn}_{11}$ Heusler Alloys

Yunli Xu¹, Dongchao Yang¹, Linjie Ding¹, Lizhi Yi¹, Shuaiwei Fan¹, Liqing Pan^{1*}, Jia Li², Fengxia Hu², Guanghua Yu³ and John Q. Xiao^{4*}

1. Research Institute for Magnetoelectronics & Weak Magnetic-field Detection,
College of Science, China Three Gorges University, Yichang 443002, China

2. State Key Laboratory of Magnetism, Institute of Physics, Chinese Academy of
Science, Beijing 100190, China

3. School of Materials Science and Engineering, University of Science and
Technology Beijing, Beijing 100083, China

4. Department of Physics and Astronomy, University of Delaware, Newark, DE,
19716, USA

Corresponding author: lpn@ctgu.edu.cn, jqx@udel.edu

Abstract: The correlation between the magnetocaloric effect and magnetotransport property was investigated in $\text{Ni}_{43}\text{Co}_7\text{Mn}_{39-x}\text{Cr}_x\text{Sn}_{11}$ Heusler alloys. Asymmetric isothermal-magnetoresistance around the phase transformation temperature were observed, from which a parameter γ , determined as a ratio of the asymmetric magnetoresistance to the temperature coefficient of resistance, is proposed. According to the Maxwell's equation, the parameter γ is analyzed to be equivalent to the transformation temperature change induced by magnetic field in martensitic transformation. This finding is confirmed with experimental results. In addition, the γ values can be used to estimate the magnetic entropy change of the martensitic transformation directly without measuring comprehensive temperature dependence of magnetization curves.

Keywords: Heusler alloy, magnetoresistance, asymmetry, magnetic-field-induced martensitic transformation

1. Introduction

Heusler alloys with magnetic-field-induced phase transformation exhibit many novel effects, such as shape memory effect induced by magnetic field [1], magnetoelastic effect [2-4], giant magnetoresistance (MR) [5], magnetocaloric effect (MCE) [6], refrigeration capacity [7], exchange bias, etc [4,8-11]. In the past decades, Ni-Co-Mn-Sn alloys have attracted much attention due to their giant MCE and giant MR effect during the phase transformation. Huang L. *et.al.* reported the entropy change of 14.9 J/Kg/K for Ni₄₀Co₁₀Mn₄₀Sn₁₀ bulk alloy under 5T [7]. For Ni₄₀Co₁₀Mn₄₀Sn₁₀ powders, it is 27 J/Kg/K reported by Wang X. L. *et.al.* [6]. Nb-doping can effectively improve the entropy change of Ni-Co-Mn-Sn alloys. For instance the entropy change reaches 41.4 J/Kg/K for Ni₄₄Nb₁Co₅Mn₄₀Sn₁₀ under 7T. Although a small amount of Nb doping can increase the entropy change of Ni-Co-Mn-Sn alloys, the latent heat of the martensitic transition decreases [12]. Large symmetric MR of -69% [13], -59% [15], -40% [14] have also been reported in Ni-Co-Mn-Sn alloys. Dubenko I. *et.al.* reported an asymmetric MR in the vicinity of the martensitic transformation, and they infer that the asymmetric MR could be related to the kinetic arrest and de-arrest of a fractional austenite phase in the martensitic transformation [17]. Samanta T. *et.al.* observed an asymmetric switching-like magnetoresistance in B-substituted Ni-Mn-In Heusler alloy, which originates from the asymmetry between the forward and reverse metamagnetic transitions[18]. Rodionov I.D. *et.al.* studied the correlation between the magnetic part of the entropy and magnetoresistance, and concluded no universal correlation between these effects[19]. In all these works, the relationship between asymmetric MR and MCE has not been studied, which is the purpose of this manuscript. We found a new parameter γ that, determined from the magnetotransport property, can be used to characterize the change of the magnetic-field-induced transformation temperature. In addition, this parameter γ can also be used to estimate the entropy changes without measuring comprehensive temperature dependence of magnetic hysteresis loops.

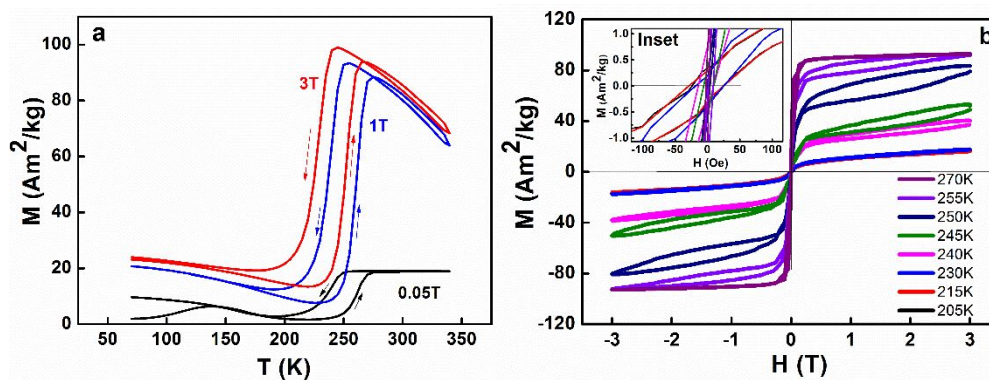
2. Experiments

Samples with nominal composition of $\text{Ni}_{43}\text{Co}_7\text{Mn}_{39-x}\text{Cr}_x\text{Sn}_{11}$, $x=0, 0.5, 1$ and 1.5 , were synthesized by arc-melting the high-purity elemental metals (Ni, 99.995%; Co, 99.95%; Mn, 99.99%; Cr, 99.999%; Sn, 99.999%) under an Ar atmosphere. The base pressure was less than 10^{-4} Pa. To compensate for the mass loss during arc melting, an excess 2 wt.% of Mn was added. All samples were melted 4–5 times under magnetic stirring, and turned over in each iteration to ensure the sample homogeneity. The obtained samples were annealed at 1173 K for 24 h in evacuated quartz tubes before quenched into an ice water bath. Finally, the obtained samples were grinded and cut into different shapes by wire cutting for testing.

The crystalline structure characterization was performed by an X-ray powder diffractometer (D8 Advance, Bruker Corp., USA) with Cu $K\alpha$ radiation. The chemical composition of the alloys was determined by energy-dispersive X-ray spectroscopy (EDS) (Quanta 200, ThermoFisher Scientific, USA). The magnetic properties and phase transformation measurements were carried out using a mini-physical property measurement system (VersaLab, Quantum Design, USA) in magnetic field up to 3T and Physical Property Measurement System (Quantum Design, USA) in magnetic field up to 7T. The MR curves were measured using the ETO mode in the VSM with standard four-probe method on sample strip of $10\text{mm}\times 2\text{mm}\times 0.5\text{mm}$.

3. Results and Discussions

3.1 MCE



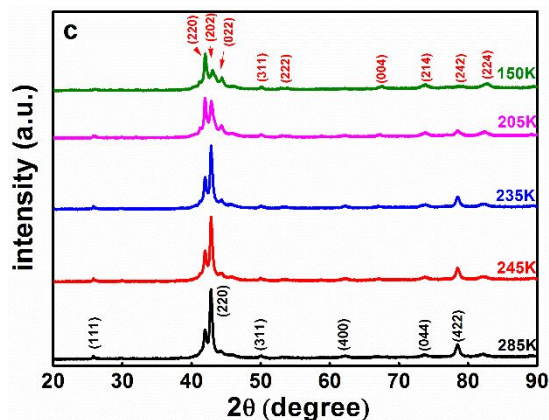


Fig.1 (a) Thermomagnetization curves of $\text{Ni}_{43}\text{Co}_7\text{Mn}_{38}\text{Cr}_1\text{Sn}_{11}$ alloy. (b) Magnetic hysteresis loops of the same alloy at different temperatures near the MT temperature. The inset is the enlarged loops near zero field. (c) Diffraction Patterns at different temperatures of the same alloy.

All samples with different Cr concentration show similar behavior. We therefore focus our discussion on a representative sample of $\text{Ni}_{43}\text{Co}_7\text{Mn}_{38}\text{Cr}_1\text{Sn}_{11}$ alloys. Fig.1(a) shows the thermomagnetization curves of the alloy. With 1% Cr dopant, the martensitic transformation starting temperature (T_M) decreases to 250K under 1T magnetic field, which is about 60K lower than that of $\text{Ni}_{43}\text{Co}_7\text{Mn}_{39}\text{Sn}_{11}$ without Cr dopant. The magnetization difference (ΔM) between the parent phase and martensite reaches $80 \text{ Am}^2/\text{kg}$ at 1T magnetic field.

The magnetic behaviors around the MT temperature can reveal the state of the magnetic order. Fig.1(b) shows the hysteresis loops of $\text{Ni}_{43}\text{Co}_7\text{Mn}_{38}\text{Cr}_1\text{Sn}_{11}$ alloy at different temperatures near the MT. The hysteresis loops below 230K show typical weak magnetic behavior, whereas the loop at 270K shows ferromagnetic behavior. The hysteresis loops exhibit obvious magnetic-field-induced metamagnetic behavior from 240K to 255K. The magnetization increases rapidly in a low field and then forms a huge hysteresis in plateau region with increasing and decreasing magnetic field. This behavior is a typical feature of the MT induced by magnetic field [20]. Note that the loops of 240K-255K are not completely closed at 3T, indicating that the Zeeman energy at 3T is not strong enough to complete the MT. The inset of Fig.1(b) shows that the coercivity is less than 50 Oe at each temperature.

The x-ray diffraction patterns (XRD) at different temperature are shown in Fig.1(c). The sample shows cubic austenite phase at 285K. With the decrease of temperature, the structure evolves into modulated martensite phase at 150K, which indicate a temperature-induced phase transformation, consistent with observed magnetic field-induced phase transformation.

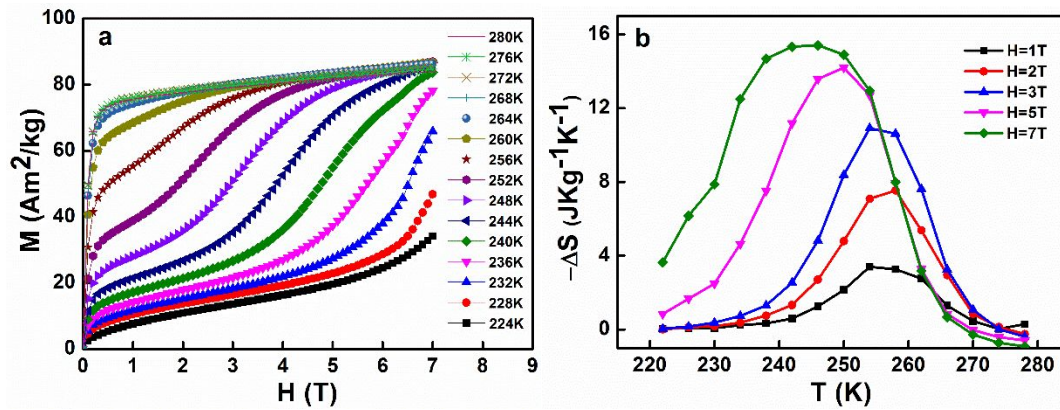


Fig.2 (a) The isothermal $M(H)$ curves at constant temperature from 224K to 280K. (b) The magnetic entropy change (ΔS) under magnetic field as a function of temperature.

Fig.2 (a) shows the isothermal $M-H$ curves measured in the vicinity of the phase transition. A large magnetic entropy change (ΔS) associated with the first-order magnetostructural transition can be calculated through the Maxwell relation based on the $M-H$ curves:

$$\Delta S = S_m(T, H) - S_m(T, 0) = \int_0^{\mu_0 H} \frac{\partial M}{\partial T} d(\mu_0 H) \quad (1)$$

Fig.2 (b) illustrates the temperature dependence of ΔS under different magnetic fields. The peak value of ΔS increases with increasing magnetic field. The maximum value of ΔS calculated under 7T is about -15.4 J/Kg/K.

3.2 Magnetotransport properties

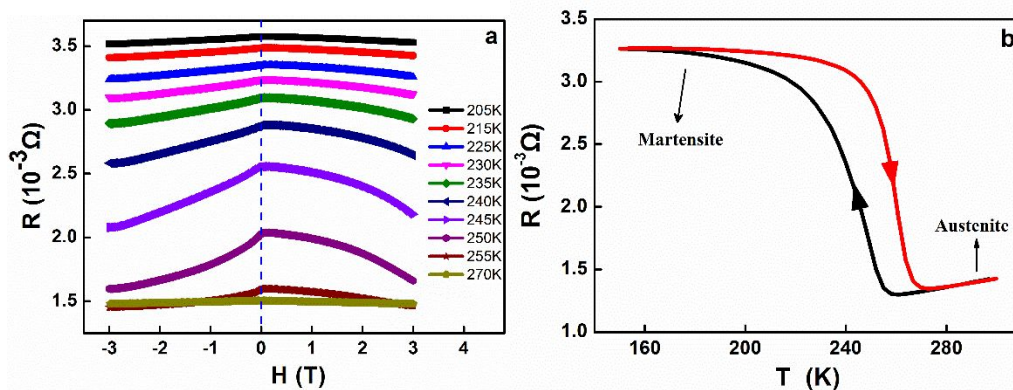


Fig.3 (a) Magnetoresistance as a function the magnetic field at different temperatures.
 (b) The temperature dependence of the resistance in zero magnetic field.

Fig.3(a) shows the MR behaviors of $\text{Ni}_{43}\text{Co}_7\text{Mn}_{38}\text{Cr}_1\text{Sn}_{11}$ alloy in magnetic field at different temperatures around the MT. For clarity we only show data in field swept from -3T to 3T, which is symmetric to those from 3T to -3T. The MR in the range of 205-230 K are nearly symmetric. As the temperature rises, the MR decreases further and the MR curves become distinctly asymmetric with respect to zero field. The resistance difference between zero and maximum fields reaches a peak at 250K, then decreases with further increasing temperature, and finally vanishes at 270K.

Fig.3(b) shows the temperature dependence of the resistance of $\text{Ni}_{43}\text{Co}_7\text{Mn}_{38}\text{Cr}_1\text{Sn}_{11}$ alloy measured at $H=0$ T. The powder XRD and TEM experiments confirmed that the parent phase has the $L2_1$ Heusler-type ordered structure with $a=0.5965$ nm, and the martensite phase is a mixture of 10M and 6M modulated structure where the crystalline structure parameters are $a=0.4319$ nm, $b=0.2747$ nm, $c=2.109$ nm, $\beta=90.64^\circ$ for 10M modulated martensite [2,24]. The distortion of the structure from cubic to monoclinic crystal during the martensitic transformation elongates the c axis of the unit cell. Consequently, the density of states at the Fermi levels decrease, which leads to the increase of the resistance as shown in Fig.3(b). The resistance loops reflect the temperature hysteresis of the MT. The red/black lines denote the heating/cooling processes, respectively. We used the cooling process to calculate the dR/dT and to measure the R - H curves.

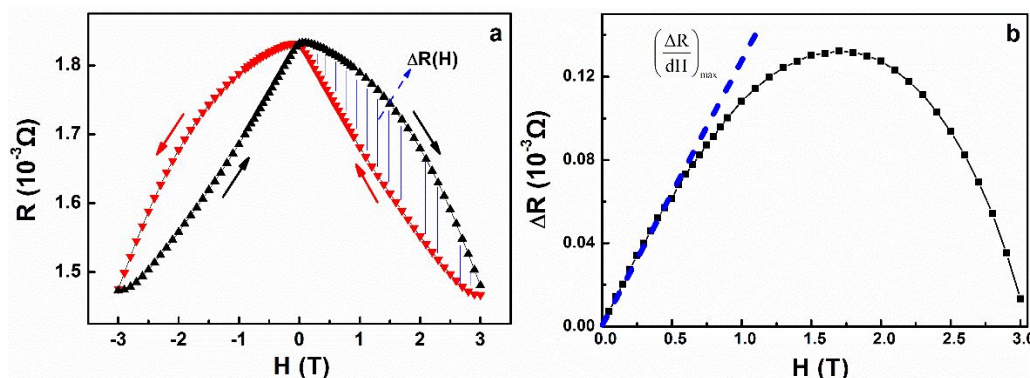


Fig.4 (a) Magnetoresistance curve at 250K. (b) Magnetic field dependence of the change of the resistance between the increasing and decreasing field (ΔR in Fig.3(a)) at 250K.

Fig.4(a) shows the magnetoresistance curve of the sample at 250K. There is a significant difference in resistance between the increasing and decreasing fields, which is related to the magnetic-field-induced phase transformation. Since the magnetic coercivity of $\text{Ni}_{43}\text{Co}_7\text{Mn}_{38}\text{Cr}_1\text{Sn}_{11}$ alloy is less than 50 Oe, the effect of magnetic hysteresis on magnetoresistance can be neglected.

3.3 Relationship between MR and MCE

The MR effect for the metamagnetic Heusler alloys near the phase transition includes two parts: the common MR and the structure-induced change of resistance by magnetic-field-induced MT effect. MR can be expressed as:

$$\Delta R = \Delta R(H) + \Delta R(S) \quad (2)$$

where $\Delta R(H)$ is the common MR without structural transformation and $\Delta R(S)$ is the resistance variation resulted from the structural change.

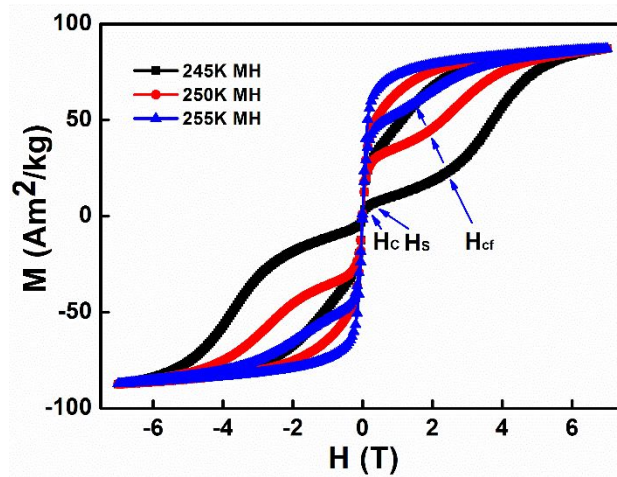


Fig.5 Magnetic hysteresis loops of $\text{Ni}_{43}\text{Co}_7\text{Mn}_{38}\text{Cr}_1\text{Sn}_{11}$ alloy at 245K, 250K, 255K, respectively. Where H_c is the coercive field, H_s is the saturation field and H_{cf} is the critical field of magnetic-field-induced phase transformation.

The unclosed hysteresis loops in Fig.1(b) indicate that the Zeeman energy in magnetic field of 3T is not big enough to complete MT for the $\text{Ni}_{43}\text{Co}_7\text{Mn}_{38}\text{Cr}_1\text{Sn}_{11}$ alloy. If the magnetic field is large enough to complete the phase transformation, the magnetization of the alloy will increase sharply as shown in Fig.5, in which we define the on-set critical field H_{cf} when the magnetization start to rise rapidly. There is a large difference between the critical field H_{cf} and the saturation field H_s , both are much larger than the coercivity H_c . In a large field range of $H_c \ll H \ll H_{cf}$, we can distinguish the origin of MR, which comes from $\Delta R(H)$ and $\Delta R(S)$. We schematically illustrate the process from negative to positive magnetic field in Fig.6.

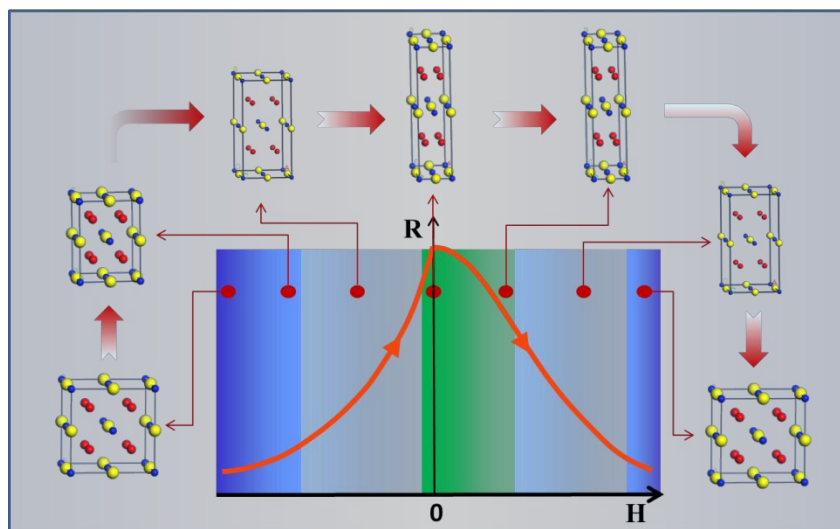


Fig.6 The schematic diagram of the $\text{Ni}_{43}\text{Co}_7\text{Mn}_{38}\text{Cr}_1\text{Sn}_{11}$ alloy structural change in magnetic field from negative to positive magnetic field.

Starting from -3T , the variation of the resistance can be expressed as $\Delta R_1 = \Delta R(H) + \Delta R(S)$, corresponding to austenite phase. Reducing the field from -3T to 0 , the Zeeman energy releases slowly and the structure of the alloy recovers gradually to the martensite phase in zero field. As the magnetic field is increased from 0 to 3T , the change of the MR undergoes two stages: (1) The Zeeman energy of small magnetic field is low, which is unable to drive any structural phase transformation. The MR only comes from single source: $\Delta R_2 = \Delta R(H)$. The spin dependent scattering decreases with increasing field, leading to the decrease of the resistance; (2) The magnetic field increases to the critical value of H_{cf} , which triggers the magnetic-field-induced inverse phase transformation, driving the structure from martensite to austenite. Therefore the MR comes from both sources and can be expressed as: $\Delta R_3 = \Delta R(H) + \Delta R(S)$. In the high field, the MR curve is gradually becoming symmetric with $\Delta R_3 = \Delta R_1$.

Since the MR is intimately related with the phase transformation, we defined a new scaling factor γ as:

$$\gamma = \left(\frac{\Delta R}{dH} \right)_{max} / \left(\frac{dR}{dT} \right) \quad (3)$$

where $\left(\frac{\Delta R}{dH} \right)_{max}$ is the asymmetric magnetoresistance, defined in Fig.4(b).

To illustrate the meaning of γ , we analyze the components of the full differential of resistance. The resistance R is a function of magnetic field H and temperature T . The full differential of $R(H, T)$ can be expressed as follow:

$$dR = \left(\frac{\partial R}{\partial T} \right)_H dT + \left(\frac{\partial R}{\partial H} \right)_T dH \quad (4)$$

or

$$\frac{dR}{dH} = \left(\frac{\partial R}{\partial T} \right)_H \frac{dT}{dH} + \left(\frac{\partial R}{\partial H} \right)_T \quad (5)$$

Therefore, the total change of resistance subtracts the change only from the magnetic field is equal to:

$$\frac{dR}{dH} - \left(\frac{\partial R}{\partial H} \right)_T = \left(\frac{\partial R}{\partial T} \right)_H \cdot \frac{dT}{dH} \quad (6)$$

The left side of Eq.(6) is the abovementioned $\left(\frac{\Delta R}{dH}\right)_{max}$. Comparing to the right side of Eq.(6), we have obtained

$$\gamma = \frac{dT}{dH} \quad (7)$$

In addition, in an adiabatic process, the change of entropy is zero.

$$dS = \left(\frac{\partial S}{\partial T}\right)_H dT + \left(\frac{\partial S}{\partial H}\right)_T dH = 0 \quad (8)$$

Therefore

$$\left(\frac{dT}{dH}\right)_S = -\frac{\left(\frac{\partial S}{\partial H}\right)_T}{\left(\frac{\partial S}{\partial T}\right)_H} \quad (9)$$

Using the Maxwell relation, we obtain:

$$\left(\frac{\partial S}{\partial H}\right)_T = \left(\frac{\partial M}{\partial T}\right)_H \quad (10)$$

Eqs. (9) and (10) lead to:

$$\left(\frac{dT}{dH}\right)_S = -\frac{\left(\frac{\partial M}{\partial T}\right)_H}{\left(\frac{\partial S}{\partial T}\right)_H} = -\left(\frac{\partial M}{\partial S}\right)_H \quad (11)$$

Which is the Clausius-Clapeyron equation [5].

Therefore, Eq.(6) can also be expressed as:

$$\frac{dR}{dH} - \left(\frac{\partial R}{\partial H}\right)_T = -\left(\frac{\partial R}{\partial T}\right)_H \left(\frac{\partial M}{\partial S}\right)_H \quad (12)$$

From Eq.(7), the γ represents the phase transformation temperature change induced by the magnetic field. It also reflects the value of $-\frac{\Delta M}{\Delta S}$ for the MT.

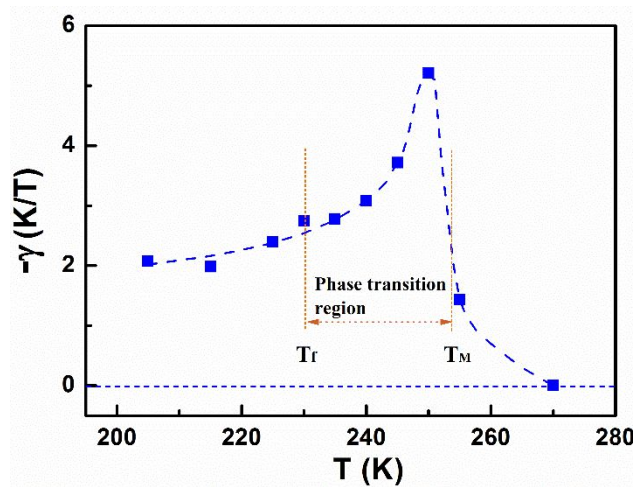


Fig.7 The temperature dependence of γ of the $\text{Ni}_{43}\text{Co}_7\text{Mn}_{38}\text{Cr}_1\text{Sn}_{11}$ alloy. T_M : martensitic transformation on-set temperature, T_f : martensitic transformation finish

temperature.

Fig.7 shows the $-\gamma$ of the $\text{Ni}_{43}\text{Co}_7\text{Mn}_{38}\text{Cr}_1\text{Sn}_{11}$ alloy calculated from Eq. (3). The value of $-\gamma$ reaches a maximum value of 5.3 K/T at 250K, and then decreases rapidly with increasing temperature and reaches zero at 270K. The value of $-\gamma$ approaches zero after the structure of the alloy has transformed into austenite, consistent with the mechanism of magnetic-field-induced phase transformation. Combined with the thermomagnetization curves in Fig.1(a), the magnetostructural-coupling phase transformation of the alloy is proved. Moreover, the value of $\frac{dT}{dH}$ can also be calculated from the transformation temperatures under the different applied magnetic fields. For instance, at $H=1\text{T}$ and $H=3\text{T}$, shown in the thermomagnetization curves in Fig.1(a), $\frac{dT}{dH} = -5\text{ K/T}$ was obtained, which is equal to the calculated value by Eq. (3).

The equivalent transformation temperature change induced by the magnetic field is generally given by the Clausius-Clapeyron equation [20]:

$$\frac{dT}{dH} = -\frac{\Delta M}{\Delta S} \quad (13)$$

where, the ΔM is the magnetization difference between the martensitic and austenite phases, and ΔS is the entropy change. From previous studies [21], the value of $-dT/dH$ is only 2 K/T for $\text{Ni}_{50}\text{Mn}_{35}\text{In}_{15}$ alloy and up to 12 K/T for $\text{Ni}_{50}\text{Mn}_{34}\text{In}_{16}$ alloy. In this work for the $\text{Ni}_{43}\text{Co}_7\text{Mn}_{38}\text{Cr}_1\text{Sn}_{11}$ alloy, the value of $-dT/dH$ is calculated to be 5.06 K/T by the Eq. (13) according to the $\Delta S = 15.4\text{ J/Kg/K}$ obtained experimentally at 7T as shown in Fig.2(b), which is very close to the $-\gamma = 5.3\text{ K/T}$ calculated by the Eq. (3). Conversely, if the values of $-\gamma$ and ΔM are known, the magnetic entropy change can be calculated directly through Clausius-Clapeyron Eq. (13), and comprehensive magnetization curves at variable temperature need not be measured except for a M-T curve taken at sufficient high magnetic field for measuring ΔM . For example, in the case of $\text{Ni}_{43}\text{Co}_7\text{Mn}_{38}\text{Cr}_1\text{Sn}_{11}$ alloy, the values of $\Delta M=78\text{ Am}^2/\text{Kg}$ and $-\gamma=5.3\text{ K/T}$ lead to $\Delta S = 14.7\text{ J/Kg/K}$ according to the Eq. (13). The value is very closer to the result of our experiment.

To verify the effectiveness of the Eq. (3), we have calculated the data in the Refs. 22, 23. The calculated γ is 5.71 (K/T). $\frac{dT}{dH} = -\frac{\Delta M}{\Delta S} = 4.85 \text{ K/T}$ is obtained from the Eq. (13), which is close to the value of γ . Since the thermomagnetization curves at 6T was not given in the Refs. 22, 23, we just use the data at 290K and 240K to calculate the ΔM . The magnitude of ΔM may be a little bit smaller than the actual value, which causes a smaller value of $\Delta M/\Delta S$. The above calculation process is detailed in the supplementary materials 2.

For samples with different Cr concentration, their compositions have been determined by EDS. The actual Co and Cr contents are about 10% smaller than the nominal composition whereas other elements slightly fluctuate around the nominal compositions. The various parameters for other samples in $\text{Ni}_{43}\text{Co}_7\text{Mn}_{39-x}\text{Cr}_x\text{Sn}_{11}$ series are shown in Table 1 (See details in Supplementary Materials). The parameter γ and dT/dH are consistent with each other.

Table 1: The magnetization of the austernite (M_A) and martensite (M_M) phases, dT/dH , are γ of all samples

Sample	M_A (emu/g)	M_M (emu/g)	dT/dH (K/T)	γ (K/T)	Origin
$\text{Ni}_{43}\text{Co}_7\text{Mn}_{39}\text{Sn}_{11}$	74	16	2.3	2.11	This work
$\text{Ni}_{43}\text{Co}_7\text{Mn}_{38.5}\text{Cr}_{0.5}\text{Sn}_{11}$	74	7.4	3.25	1.97	This work
$\text{Ni}_{43}\text{Co}_7\text{Mn}_{38}\text{Cr}_1\text{Sn}_{11}$	98	20	5.0	5.3	This work
$\text{Ni}_{43}\text{Co}_7\text{Mn}_{37.5}\text{Cr}_{1.5}\text{Sn}_{11}$	106	53	6.6	6.4	This work
$\text{Ni}_{42}\text{Co}_8\text{Mn}_{32}\text{Al}_{18}$	/	/	4.85	5.71	Ref.22,23

4. Conclusions

The relationship between asymmetric MR and MCE has been studied by Maxwell relation and Clausius-Clapeyron equations, and verified experimentally. In the vicinity of the phase transformation of the $\text{Ni}_{43}\text{Co}_7\text{Mn}_{39-x}\text{Cr}_x\text{Sn}_{11}$ alloys, the asymmetric MR has been observed, which corresponds to the magnetostructural transformation. We propose a new factor γ , which can be determined from the magnetotransport properties, and prove it is equivalent to the transformation

temperature change induced by magnetic field. This factor γ can also be used to estimate the magnetic entropy of the martensitic transformation.

Acknowledgement:

The author of Y.L.Xu thanks Mr. Cheng Chen for the help in the magneto-transport measurement. This work was supported by National Natural Science Foundation of China (Grant Nos.: 51371105, 11474183 and 51501102), J.Q.X. is supported by NSF grant DMR1505592.

References:

- [1] Chen, F., Tong, Y. X., Tian, B., Li, L. and Zheng, Y. F., Martensitic transformation and magnetic properties of Ti-doped NiCoMnSn shape memory alloy, *Rare Met.*, 2014, **33**(5), 511-515.
- [2] Kainuma, R., Imano, Y., Ito, W., Morito, H., Sutou, Y., Oikawa, K., Fujita, A., Ishida, K., Okamoto, S., Kitakami, O. and Kanomata, T., Metamagnetic shape memory effect in a Heusler-type Ni₄₃Co₇Mn₃₉Sn₁₁ polycrystalline alloy, *Appl. Phys. Lett.*, 2006, **88**, 19.
- [3] Bruno, N. M., Yegin, C., Karaman, I., Chen, J.-H., Ross, J. H., Liu, J. and Li, J., The effect of heat treatments on Ni₄₃Mn₄₂Co₄Sn₁₁ meta-magnetic shape memory alloys for magnetic refrigeration, *Acta Mater.*, 2014, **74**(4), 66-84.
- [4] Yang, Z., Cong, D. Y., Huang, L., Nie, Z. H., Sun, X. M., Zhang, Q. H. and Wang, Y. D., Large elastocaloric effect in a Ni–Co–Mn–Sn magnetic shape memory alloy, *Mater. Design*, 2015, **92**, 932-936.
- [5] Yu, G. H., Xu, Y. L., Liu, Z. H., Qiu, H. M., Zhu, Z. Y., Huang, X. P., Pan, L. Q., Recent progress in Heusler-type magnetic shape memory alloys. *Rare Met.*, 2015, **34**, 527-539.
- [6] Wang, X., Sun, F., Wang, J., Yu, Q., Wu, Y., Hua, H. and Jiang, C., Influence of annealing temperatures on the magnetostructural transformation and magnetocaloric effect of Ni₄₀Co₁₀Mn₄₀Sn₁₀ powders, *J. Alloy. Compd.*, 2017, **691**, 215-219.
- [7] Huang, L., Cong, D. Y., Suo, H. L. and Wang, Y. D., Giant magnetic refrigeration capacity near room temperature in Ni₄₀Co₁₀Mn₄₀Sn₁₀ multifunctional alloy, *Appl. Phys. Lett.*, 2014, **104**(13), 132407.
- [8] Halder, M., Mukadam, M. D., Suresh, K. G. and Yusuf, S. M., Electronic, structural, and magnetic properties of the quaternary Heusler alloy NiCoMnZ (Z=Al, Ge, and Sn), *J. Magn. Mater.*, 2015, **377**, 220-225.
- [9] Çakır, A., Acet, M., Wiedwald, U., Krenke, T., Farle, M., Shell-ferromagnetic precipitation in martensitic off-stoichiometric Ni-Mn-In Heusler alloys produced by temper-annealing under magnetic field, *Acta Mater.*, 2017, **127**, 117-123.
- [10] Srivastava, V., Chen, X. and James, R. D., Hysteresis and unusual magnetic properties in the singular Heusler alloy Ni₄₅Co₅Mn₄₀Sn₁₀, *Appl. Phys. Lett.*, 2010, **97**(1), 159.

- [11] Ma, S. C., Xuan, H. C., Zhang, C. L., Wang, L. Y., Cao, Q. Q., Wang, D. H. and Du, Y. W., Investigation of the intermediate phase and magnetocaloric properties in high-pressure annealing Ni–Mn–Co–Sn alloy, *Appl. Phys. Lett.*, 2010, **97**(5), 1746.
- [12] Emre, B., Bruno, N. M., Yuce, E. S. and Karaman, I., Effect of niobium addition on the martensitic transformation and magnetocaloric effect in low hysteresis NiCoMnSn magnetic shape memory alloys, *Appl. Phys. Lett.*, 2014, **105**, 23.
- [13] Ghosh, A., Mandal, K., Large magnetoresistance associated with large inverse magnetocaloric effect in Ni-Co-Mn-Sn alloys, *Eur. Phys. J. B.*, 2013, **86**(9), 1-6.
- [14] Liu, Z. H., Wu, Z. G., Ma, X. Q., Wang, W. H., Liu, Y., Wu, G. H., Large magnetization change and magnetoresistance associated with martensitic transformation in $\text{Mn}_2\text{Ni}_{1.36}\text{Sn}_{0.32}\text{Co}_{0.32}$ alloy, *J. Appl. Phys.*, 2011, **110**(1), 957.
- [15] Han, Z. D., Wang, D. H., Qian, B., Feng, J. F., Jiang, X. F., Du, Y. W., Phase Transformations, Magnetocaloric Effect and Magnetoresistance in Ni-Co-Mn-Sn Ferromagnetic Shape Memory Alloy, *Jpn. J. Appl. Phys.*, 2010, **49**(1), 0211.
- [16] Graf, T., Felser, C. and Parkin, S.S.P., Simple rules for the understanding of Heusler compounds, *Prog. Solid State Chem.*, 2011, **39**, 1-50.
- [17] Dubenko, I., Samanta, T., Quetz, A., Saleheen, A., Prudnikov, V. N., Granovsky, A. B., Stadler, S., Ali, N., Asymmetric magnetoresistance in bulk In-based off-stoichiometric Heusler alloys. *Phys. Status Solidi (c)*, 2014, **11**(5-6), 1000-1003.
- [18] Samanta, T., Saleheen, A. U., Lepkowski, D. L., Shankar, A., Stadler, S., Asymmetric switchinglike behavior in the magnetoresistance at low fields in bulk metamagnetic heusler alloys. *Phys. Rev. B*, 2014, **90**(6), 064412.
- [19] Rodionov, I. D., Mettus, D. E., Kazakov, A. P., Prudnikova, M. V., Prudnikov, V. N., Dubenko, I. S., et al., Correlation between magnetoresistance and magnetic entropy at first-order and second-order phase transitions in ni-mn-in-si heusler alloys. *Physics of the Solid State*, 2013, **55**(9), 1861-1865.
- [20] Kainuma, R., Imano, Y., Ito, W., Sutou, Y., Morito, H., Okamoto, S., Kitakami, O., Oikawa, K., Fujita, A., Kanomata, T. and Ishida, K., Magnetic-field-induced shape recovery by reverse phase transformation, *Nature*, 2006, **439**, 7079.
- [21] Yu, S. Y., Liu, Z. H., Liu, G. D., Chen, J. L., Cao, Z. X., and Wu, G. H., Large

magnetoresistance in single-crystalline $\text{Ni}_{50}\text{Mn}_{50-x}\text{In}_x$ alloys ($x=14-16$) upon martensitic transformation, *Appl. Phys. Lett.*, 2006, **89**, 162503.

[22] Xuan, H. C., Shen, L. J., Tang, T., Cao, Q. Q., Wang, D. H., and Du, Y. W., Magnetic-field-induced reverse martensitic transformation and large magnetoresistance in $\text{Ni}_{50-x}\text{Co}_x\text{Mn}_{32}\text{Al}_{18}$ Heusler alloys, *Appl. Phys. Lett.*, 2012, **100**, 172410.

[23] Xuan, H. C., Chen, F. H., Han, P. D., Wang, D. H., Du, Y. W., Effect of Co addition on the martensitic transformation and magnetocaloric effect of Ni-Mn-Al ferromagnetic shape memory Alloys, *Intermetallics*, 2014, **47**, 31-35.

[24] Morito, S., Kakeshita, T., Hirata, K., Otsuka, K., Magnetic and martensitic transformations in $\text{Ni}_{50}\text{Al}_x\text{Mn}_{50-x}$ alloys, *Acta Mater.*, 1998, 46(15):5377-5384.